

# Recovering noise-free quantum observables

Matthew Otten and Stephen Gray

*Center for Nanoscale Materials, Argonne National Laboratory, Lemont, Illinois, 60439*

(Dated: June 21, 2018)

We introduce a technique for recovering noise-free observables in noisy quantum systems by combining the results of many slightly different experiments. Our approach is applicable to a variety of quantum systems but we illustrate it with applications to quantum computing and quantum sensing. The approach corresponds to repeating the same quantum evolution many times with known variations on the underlying systems' error properties, e.g. the spontaneous emission and dephasing times,  $T_1$  and  $T_2$ . As opposed to standard quantum error correction methods, which have an overhead in the number of qubits (many physical qubits must be added for each logical qubit) our method has only an overhead in number of evaluations, allowing the overhead to, in principle, be hidden via parallelization. We show that the effective spontaneous emission,  $T_1$ , and dephasing,  $T_2$ , times can be increased using this method in both simulation and experiments on an actual quantum computer. We also show how to correct more complicated entangled states and how Ramsey fringes relevant to quantum sensing can be significantly extended in time.

Quantum information science is rapidly evolving due to advances in quantum computing, communication, and sensing. Quantum computing, for example, has the possibility to show exponential speedup in areas such as prime number factoring [1] and quantum chemistry [2] and quantum sensing has the potential to be able to be far more sensitive than classical sensing [3]. However, in all quantum information applications, decoherence (or information loss) is a serious problem in advancing beyond elementary demonstrations. Quantum error correction is a way to extend the lifetime of quantum information by encoding a single logical qubit into many physical qubits [4]. This introduces both space and time overheads owing to the additional number of physical qubits required and the additional gate operations. Furthermore, it is not clear how standard quantum error correction could be used in complicated quantum sensors.

In this Letter, we describe a technique for recovering observables from a quantum evolution by repeating the evolution with slightly different noise characteristics and combining those results to obtain an estimate of the noise-free answer without the need of additional quantum hardware. Our approach bares some similarities with interesting recent work by Gambetta and coworkers [5, 6] involving one noise parameter, a simple model for observable variation with error, and Richardson extrapolation. The approach we develop may be viewed as a multi-dimensional generalization not reliant on Richardson extrapolation. We should note that we have recently used such a simple error model to develop a different error correction scheme that requires the ability to significantly reduce error on individual qubits via, e.g., quantum error correction [7]. The approach presented here, which does not rely on quantum error correction, requires many, slightly different runs to be completed; these can be done in time (repeating the evolution many times in sequence) or in parallel (many separate quantum systems undergo the same evolution at the same time). The abil-

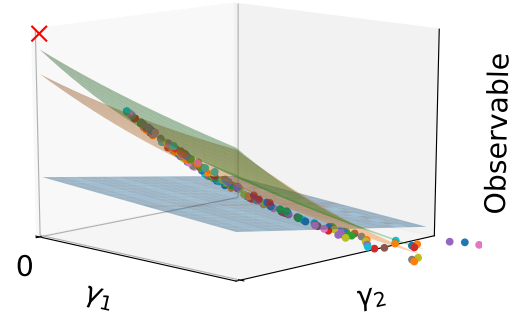


FIG. 1: An example of a ‘hypersurface’ fit to many experiments with slightly different noise parameters,  $\gamma_1$  and  $\gamma_2$ . The red ‘X’ represents the noise-free observable. The blue, orange, and green surfaces are first, third, and fourth order fits, respectively. Note that this plot is zoomed; many other observable measurements are outside of the visible region.

ity to trade overhead between space and time also has advantages over standard quantum error correction. Our approach can be used in quantum algorithms, quantum sensing, and even general quantum experiments where the decoherence time is too short to obtain high-quality signals. The only requirement is that the evolution can be repeated with different, well-characterized noise sources.

Consider a quantum system with one or more subsystems (e.g., qubits), each undergoing a small set of dominant noise processes parameterized by a set of noise rates  $\{\gamma_i\}$ . Suppose that this system repeatedly undergoes a given evolution (such as a sequence of quantum gates or interaction with a magnetic field) with varying values of

the noise rates  $\{\gamma_i\}$ . These repetitions can be accomplished sequentially on one system (consuming time) or in parallel on a set of systems (consuming space) or in some combination. Combining all results, we construct a hypersurface embedded in a space where one axis represents the results of a measurement and each of the other axes represent the effect of a noise rate parameter. The form of the hypersurface is obtained via the Taylor expansion of the quantum system's evolution operator (see Appendix). This hypersurface yields an estimate of the noise-free observable and gives general information about the effect of each noise rate.

To be concrete, consider a single qubit with only amplitude damping noise. We repeatedly apply some evolution to this qubit, but each time the noise rates are different. Let  $\gamma_1^{[j]}$  be the amplitude damping rate for the  $j$ th repetition and  $\langle A \rangle^{[j]}$  be the corresponding measured observable. Restricting our observable model to third order in  $\gamma_1$ , we would solve (by standard least-squares procedures)

$$\begin{bmatrix} 1 & \gamma_1^{[1]} & (\gamma_1^{[1]})^2 & (\gamma_1^{[1]})^3 \\ 1 & \gamma_1^{[2]} & (\gamma_1^{[2]})^2 & (\gamma_1^{[2]})^3 \\ 1 & \gamma_1^{[3]} & (\gamma_1^{[3]})^2 & (\gamma_1^{[3]})^3 \\ \vdots & \vdots & \vdots & \vdots \end{bmatrix} \begin{bmatrix} A_0 \\ A_1 \\ A_{11} \\ A_{111} \end{bmatrix} = \begin{bmatrix} \langle A \rangle^{[1]} \\ \langle A \rangle^{[2]} \\ \langle A \rangle^{[3]} \\ \vdots \end{bmatrix}, \quad (1)$$

to obtain  $(A_0, A_1, A_{11}, A_{111})$  and the observable as a function of the noise rate is given by  $\langle A \rangle \approx A_0 + A_1\gamma_1 + A_{11}\gamma_1^2 + A_{111}\gamma_1^3$ . In this case the hypersurface is just a cubic curve with intercept  $A_0$  being the desired noise-free value. The formalism easily extends to higher orders and to many noise parameters, potentially from many qubits. For example, using a single qubit with a spontaneous emission rate,  $\gamma_1$  and pure dephasing rate,  $\gamma_2$ , the  $j$ th row of our matrix would be  $[1 \ \gamma_1^{[j]} \ \gamma_2^{[j]} \ (\gamma_1^{[j]})^2 \ \gamma_1^{[j]}\gamma_2^{[j]} \ (\gamma_2^{[j]})^2]$ , where we truncate to second order. Figure 1 displays hypersurfaces (now 2D surfaces) for such a system with two noise parameters. A red 'X' is the noise-free solution. As model order is increased, the surfaces better fit the data and extrapolate closer to the noise-free limit. For many qubits with many noise rates, the result is a high-dimensional hypersurface.

We first demonstrate this method for a single qubit using a simple relaxation time experiment. We excite the qubit into the  $|1\rangle$  state, wait some amount of time, and then measure what state it is in; repeating this many times allows a probability of remaining in (or fractional population of) the excited state to be obtained. Without noise, each measurement result (and the fractional population of the excited state) would be unity for all times. Due to the amplitude damping noise, the population will decay to zero with characteristic time  $T_1$ . We first show this in simulation, where we select random  $\gamma_1$  values uniformly in a range representing  $T_1$  times between  $5 \mu\text{s}$  and  $15 \mu\text{s}$ . All simulations are numerical solutions of

the Lindblad master equation [8, 9] and utilize the high-performance open quantum systems solver QuaC [10]. The results are shown in Fig. 2a, where we plot the best, worst, and average evolutions over 450 repetitions, and the recovered populations using equation (1), up to tenth order. The procedure is applied at specific times, with knowledge only of the measured observables at that time. By recovering at many different times  $t$ , we obtain the full evolution. Every order, from first until tenth, is better than the best run; increasing the order increases the quality of the recovery. Take, for example, the value of the observable at  $60 \mu\text{s}$ . At this point, the average population is 0.0045; essentially all of the state has decayed away. The first order recovery gives a population of only 0.017. The tenth order recovery gives a population of 0.90, which is nearly the noise-free result. Defining an effective  $T_1(n)$  for a given order  $n$  as the time the recovered evolution has  $1/e$  population remaining, we see  $T_1(n) \approx (n+1)T_1(n=0)$ .

We also perform the relaxation time experiment on Rigetti's eight qubit chip, Agave [11, 12], a superconducting qubit quantum computer with a ring topology. Each of the eight qubits has slightly different  $T_1$  and  $T_2^*$  times, all approximately  $10 \mu\text{s}$ . Furthermore, these noise characteristics drift in time [6, 13]. These features provide the necessary variation in noise parameters for our method. We first excite a single qubit using a Pauli-X gate, wait some time, and measure the qubit state. This is repeated for many different wait times. Each experiment at a given wait time is averaged over  $10^5$  shots, giving an average population. The  $T_1$  time and associated decay rate,  $\gamma_1$ , is extracted by fitting an exponential to the data. This process is repeated for each qubit in the eight qubit chip, a few minutes are allowed to pass, and then the full cycle is repeated, starting from the first qubit. This generates many different repetitions with varying noise parameters. The fitted  $\gamma_1$  parameters are used for the recovery method. Just as in the simulation, each wait time is recovered separately. A total of 45 different single qubit repetitions are run with results shown in Fig. 2b. Both first and second order recoveries result in a higher population than the average, similar to the simulation results. The recovery is limited by noise sources not included in the model, such as readout noise. Neither first nor second order recovery reaches the correct value of 1; instead, they recover  $\approx 0.9$ , roughly the average readout fidelity of the qubits used in the experiment.

With only one noise parameter the method is very similar to Richardson extrapolation, which has been shown to be able to extrapolate to the zero-noise limit in superconducting qubits [5, 6]; mathematically, the methods differ only in the choice of points and specific fitting strategy, but the source of the variation in noise differs greatly. The Richardson extrapolation technique assumes a single global noise source, implemented by scaling the length of the pulses while running the quantum algorithm on the

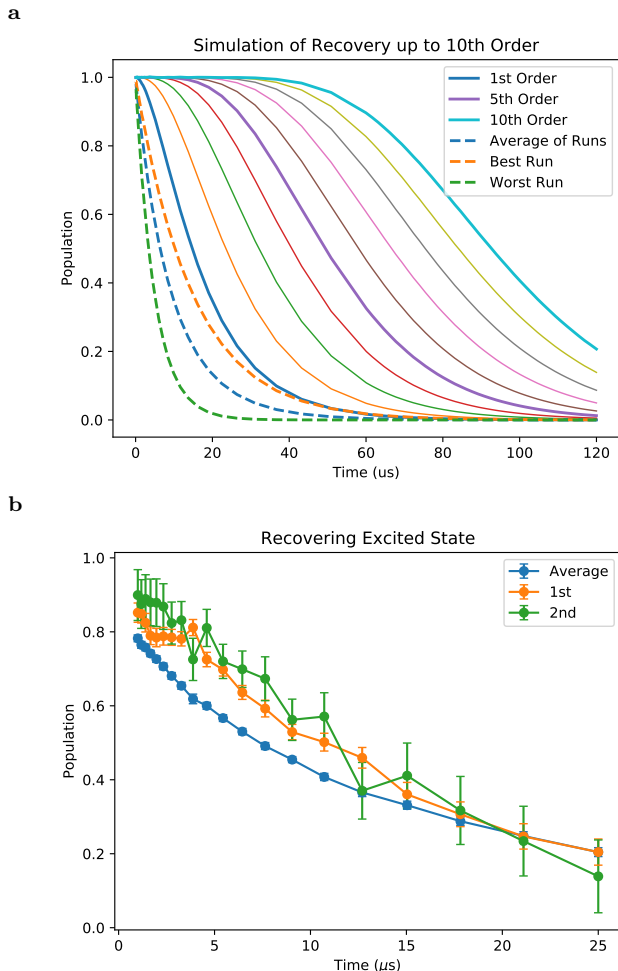


FIG. 2: Recovery of the population in a relaxation time experiment. (a) Simulated data from 450 simulations with random  $T_1$  times. (b) Experimental results on Rigetti's 8 qubit quantum computer, Agave [11]. 45 separate repetitions are made at each time with experimentally determined  $T_1$  times.

same set of qubits [6]. The hypersurface method allows for any number of noise sources and can be thought of as a multi-dimensional generalization which utilizes the natural variations in qubit properties. To show this, we use Ramsey interferometry with no background magnetic field, a common technique for measuring  $T_2$  times [14]. This involves applying a  $\pi/2$   $X$  rotation to  $|0\rangle$ , waiting some time, and then applying another  $\pi/2$   $X$  rotation. Without noise and in a rotating frame, the final state would be  $|1\rangle$ . As opposed to the relaxation time experiment, both the amplitude damping and dephasing noise affect the result. Figure 3a shows simulated results of this experiment with recovery up to 8th order. Spontaneous emission  $T_1$  and pure dephasing  $T_2^*$  times are independently, randomly chosen between 5  $\mu$ s and 15  $\mu$ s with 450 simulations being run. Without recovery, the ex-

cited state population associated with a given  $\gamma_1 = 1/T_1$  and  $\gamma_2 = 1/T_2^*$  exponentially decays in time with rate  $1/T_2 = \gamma_1/2 + \gamma_2$ . As with the relaxation time experiments, first order recovery leads to a better evolution for most points compared with even the best run of all the qubits. As ever higher orders are considered, a unity excited state population is recovered for longer periods of time.

We also carry out Ramsey experiments on Rigetti's eight qubit Agave quantum computer. To obtain the correct noise rates,  $\gamma_i$ , for a given repetition we first characterize  $T_1$  using the relaxation time experiment discussed above. We then perform a Ramsey interferometry experiment as previously described. The results of this experiment are fit to an exponential to obtain  $T_2$ . This allows determination of the pure dephasing rate via  $\gamma_2 = 1/T_2 - 1/(2T_1)$ . Each wait time in both the  $T_1$  and  $T_2$  determinations is averaged over  $10^5$  shots. With both necessary rates determined, the hypersurface method, equation (1), is used to recover the excited state population at each wait time, using 12 repetitions (Fig. 3b). The first order correction recovers a significant fraction of the missing population and approaches the readout fidelity limit at early times.

Characterization of the noise rates and a good understanding of the important noise sources is imperative for this method. For example, because of the way  $\gamma_2$  is determined, poor determinations of  $T_1$  and  $T_2$  can sometimes lead to negative  $\gamma_2$ ; these unphysical repetitions are excluded from the recovery in our experiments. In both experiments on the Rigetti quantum computer, the correct unity excited state population could not be recovered. Instead, the method recovered the readout fidelity limit. In superconducting qubit systems, where noise fluctuates over time scales in the few minute range,  $T_1$  and  $T_2$  would need to be characterized before essentially every repetition to ensure that the hypersurface equations have the correct noise sources.

The Ramsey experiments show the strength of this method, compared to Richardson extrapolation with a global noise parameter. Rather than stretching out the circuit, limiting the number of logical gates that can be done, our method involves determination of the noise parameters (in this case,  $T_1$  and  $T_2^*$  times), followed by evaluation of the relevant algorithm or experiment. Furthermore, this can be done in parallel. In superconducting circuits, each qubit has slightly different noise characteristics. Our method allows these different noise characteristics to be utilized for the recovery of the observable. For example, several small quantum computers could be produced and an algorithm could be evaluated in parallel. At the end, the results could be combined to give approximate noise-free observables. The overhead of the method can be paid in either time or space. If the quantum computer is much larger than the number of logical qubits needed for a given algorithm, the extra qubits can

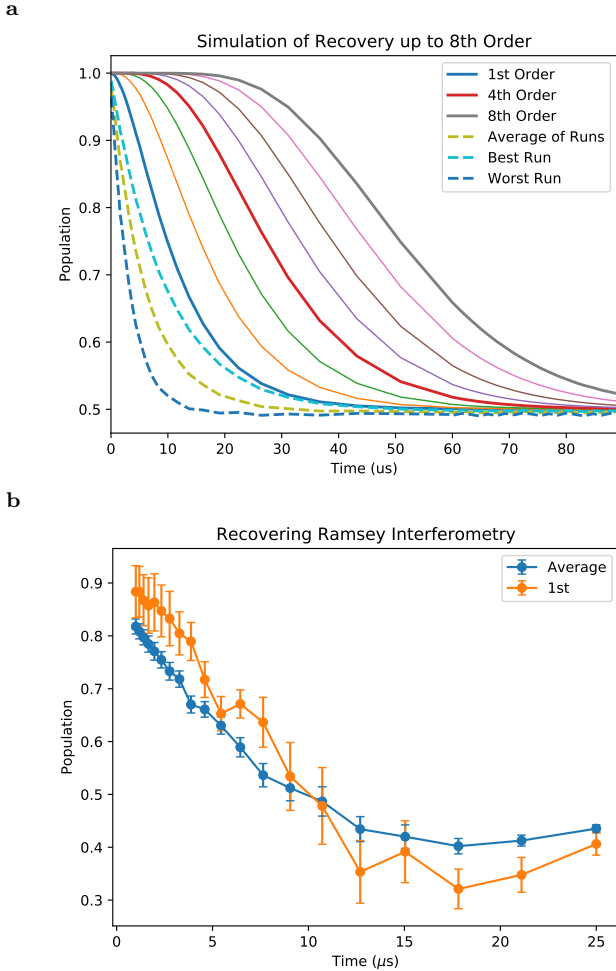


FIG. 3: Recovery of population in Ramsey interferometry experiment with no background magnetic field. (a) Simulated data from 450 simulations with random  $T_1$  and  $T_2^*$  times. (b) Experimental results on Rigetti's 8 qubit quantum computer, Agave [11]; 12 separate repetitions are included at each time, with experimentally determined  $T_1$  and  $T_2^*$  times.

be used to run the same algorithm in parallel. Alternatively, the algorithm can be run many times in succession; here, the noise characteristics can be changed by waiting for natural fluctuations, by changing the logical to physical qubit mapping, or by carefully tuning the noise (if the quantum hardware allows that). By utilizing a single global noise source, the Richardson extrapolation technique generally requires many fewer evaluations than the hypersurface method; however, these evaluations must be done before the natural fluctuations of the underlying noise parameters change. Furthermore, in quantum sensors and general quantum experiments, it can be infeasible to stretch out the evolution; the hypersurface method only requires the same evolution to be repeated.

As a final example, we perform a simulation of Ram-

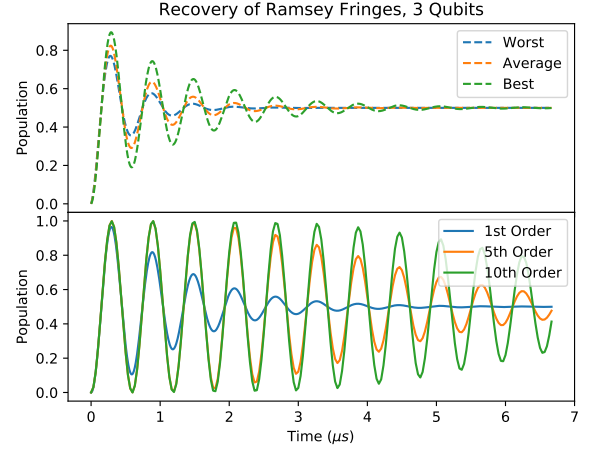


FIG. 4: Recovery of Ramsey fringes from entangled qubits using 350 simulations of three qubits with random  $T_2^*$  times.

sey interferometry with a background magnetic field. This is a common technique used in quantum sensing of magnetic fields [3]. Both single qubit and entangled arrays of qubits can be used as sensors [15]. The system is first prepared in a superposition state such as  $\frac{1}{\sqrt{2}}(|0\rangle + |1\rangle)$  in the case of a single qubit sensor and the GHZ state,  $\frac{1}{\sqrt{2}}(|00\dots 0\rangle + |11\dots 1\rangle)$ , for an entangled array of qubits [3]. Single qubit superposition states can be prepared with a Hadamard gate; GHZ states can be prepared with a Hadamard gate and a sequence of CNOT gates. The system then evolves in the presence of a background magnetic field, causing it to pick up a phase. The inverse entangling operation is then applied, transferring the phase onto a single qubit, which is then measured. The phase accumulated over the course of the interaction depends on the strength of the magnetic field and the time the system interacts with it. If the interaction time is too much longer than the coherence time, all of the useful information decays away, and the characteristic Ramsey fringes will no longer be visible. We simulate this experiment using both a single qubit and three entangled qubits. For each qubit, we select a random  $T_2^*$  times in the range of  $0.5\mu\text{s}$  to  $1.5\mu\text{s}$ , consistent with parameters for nitrogen-vacancy centers [16]. The characteristic  $T_1$  time is large enough to be safely ignored. We set the background magnetic field to  $10\mu\text{T}$  and use a total of 350 samples for both the single qubit and entangled qubit simulations. Figure 4 shows the recovery of Ramsey fringes from a three qubit GHZ state; the single qubit case is plotted in the Appendix. In the three qubit case we now have three noise parameters, one for each qubit. The higher order recovery now involves many cross terms, and the resulting hypersurface is three-dimensional. Even in this maximally entangled

state, the Ramsey fringes are still recovered long after most of the individual fringes have decayed away.

We presented a novel method to recover arbitrary quantum observables by repeatedly measuring the observables with differing noise rates and fitting a hypersurface to the repetitions. By including more and more repetitions and increasing the hypersurface order, an increasingly good approximation of noise-free observables of general quantum system can be recovered. For many quantum systems,  $T_1$  and  $T_2^*$  noise are the dominant noise sources and there are many techniques for characterizing them. Our method can recover a good approximation of the noise-free evolution in these cases. As shown in this Letter, this method has applications in quantum computing and quantum sensing. Further study on ways to minimize the number of repetitions needed for higher-order recovery of a large number of coupled quantum systems is necessary to control the overhead of the method. Demonstrations of more complicated algorithms and larger numbers of coupled quantum systems is also warranted.

This work was performed at the Center for Nanoscale Materials, a U.S. Department of Energy Office of Science User Facility, and supported by the U.S. Department of Energy, Office of Science, under Contract No. DE-AC02-06CH11357. We gratefully acknowledge the computing resources provided on Bebop, a high-performance computing cluster operated by the Laboratory Computing Resource Center at Argonne National Laboratory. We thank Rigetti Computing for use of the Agave quantum computer, and Guenevere Prawiroatmodjo for help in setting up the experiments on Agave.

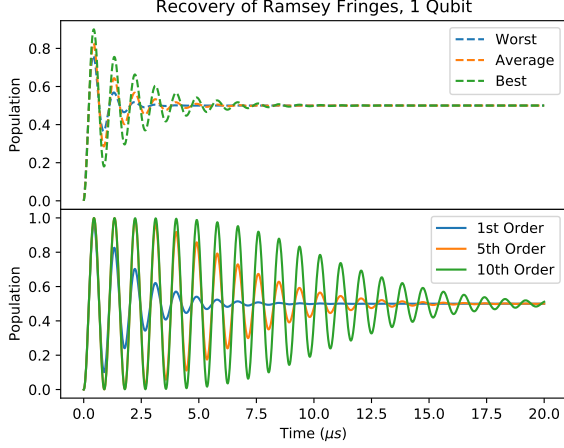


FIG. 5: Single qubit Ramsey interferometry. 350 simulations with random  $T_2^*$  times are used.

## Appendix

### Recovery of Single Qubit Ramsey Fringes

Figure 5 shows the recovery of Ramsey fringes for a single qubit. In this single qubit case, there is only one noise parameter,  $\gamma_2$ , as  $\gamma_1 \ll \gamma_2$ , in contrast to the Ramsey interferometry in the superconducting qubit system, where  $\gamma_1 \approx \gamma_2$ . We set the background magnetic field to 10  $\mu\text{T}$  and combine the results of 350 experiments. As the order of the recovery is increased, more and more fringes are recovered; at tenth order, the fringes extend are recovered even when the best single qubit run has no clearly visible fringes. Without correction, the fringes decay with the characteristic  $T_2$  time [14].

### Derivation

The Lindblad master equation for a general density matrix  $\rho(t)$  evolved from an initial state  $\rho_0$  is defined as (throughout,  $\hbar = 1$ )

$$\frac{d\rho}{dt} = -i[H, \rho_0] + L(\rho_0), \quad (2)$$

where  $H$  is the Hamiltonian of the system, describing coherent evolution and  $L$  is the Lindblad superoperator, describing incoherent evolution, such as noise processes. Both  $H$  and  $L$  can, generally, be time dependent. ‘Vectorizing’ the density matrix [17],  $\rho$ , allows us to write a general solution of the Lindblad master equation as

$$\tilde{\rho}(t) = \exp(-i\tilde{H}t + \tilde{L}t)\tilde{\rho}_0, \quad (3)$$

where  $\tilde{\rho}$  is the vectorized density matrix,  $\tilde{H}$  is the vectorized Hamiltonian, and  $\tilde{L}$  is the vectorized Lindblad superoperator. See Ref. 17 for more details about the process of vectorization. We can decompose the exponential in the solution, equation (3), using the Trotter decomposition [18]:

$$\exp(-i\tilde{H}t + \tilde{L}t) = \lim_{n \rightarrow \infty} \left( \left( \exp(-i\tilde{H}\frac{t}{n}) \exp(\tilde{L}\frac{t}{n}) \right)^n \right) \quad (4)$$

and take the Taylor expansion of the exponential of the Lindblad

$$\exp(-i\tilde{H}t + \tilde{L}t) = \lim_{n \rightarrow \infty} \left( \left( \exp(-i\tilde{H}\frac{t}{n}) \sum_{m=0}^{\infty} \frac{(\tilde{L}\frac{t}{n})^m}{m!} \right)^n \right). \quad (5)$$

We now write the Lindblad superoperator as a sum of many different Lindblad superoperators, each with its own rate:  $\tilde{L} = \sum_j \gamma_j \tilde{L}_j$  and plug this into equation (5), giving

$$\exp(-i\tilde{H}t + \tilde{L}t) = \lim_{n \rightarrow \infty} \left( \left( \exp(-i\tilde{H}\frac{t}{n}) \sum_{m=0}^{\infty} \frac{(\sum_j \gamma_j \tilde{L}_j \frac{t}{n})^m}{m!} \right)^n \right). \quad (6)$$

Equation (6) an infinite sum over  $m$ , a finite sum over  $i$ , and is raised to an infinite power,  $n$ . Though this equation has infinite terms, we can collect all terms that have the same  $\gamma$  prefactors. For example, the collection of all terms with only  $\gamma_j$  will include all terms from the product that have one first order element from the Taylor series expansion of  $\tilde{L}$ . Terms with  $\gamma_j^2$  will include products with two first order elements, as well as products with one second order element. To provide a concrete example, we truncate the Trotterization at third order, the Taylor expansion at first order, and include two noise terms. Let  $U = \exp(-i\tilde{H}\frac{t}{3})$  and  $V_j = \tilde{L}_j \frac{t}{3}$ . With our truncation, we rewrite equation (6) as

$$\begin{aligned} \exp(-i\tilde{H}t + \tilde{L}t) &\approx \left( U(1 + \gamma_1 V_1 + \gamma_2 V_2) \right)^3 \\ &\approx UUU + \gamma_1(UV_1UU + UUV_1U + UUV_1U) + \gamma_2(UV_2UU + UUV_2U + UUV_2U) + \\ &\quad + \gamma_1^2(UV_1UV_1U + UUV_1UV_1 + UV_1UUV_1) + \gamma_2^2(UV_2UV_2U + UUV_2UV_2 + UV_2UUV_2) \\ &\quad + \gamma_1\gamma_2(UV_1UV_2U + UUV_1UV_2 + UV_1UUV_2 + UV_2UV_1U + UUV_2UV_1 + UV_2UUV_1). \end{aligned} \quad (7)$$

The generalization to higher order Trotterizations is clear; the expanded sum will have many more terms (due to each term having a smaller timestep,  $\frac{t}{n}$ ), but terms can be grouped by their  $\gamma_j$  prefactors. For higher order Taylor expansions of  $\exp \tilde{L}$ , terms can still be grouped by their  $\gamma_j$  prefactors. For example, take the  $\gamma_1^2$  term from equation (7). With a second order Taylor expansion, the  $\gamma_1^2$  terms now contain contributions from  $V_1^2$ :

$$[\gamma_1^2 \text{ terms}] = UV_1UV_1U + UUV_1UV_1 + UV_1UUUV_1 + UV_1^2UU + UUV_1^2U + UUV_1^2 \quad (8)$$

Combining the generalizations to both higher order Trotterization and higher order Taylor expansion is relatively straightforward; the number of terms grows precipitously, but they can always be gathered by their  $\gamma_j$  prefactors. Collecting all the terms for both the infinite limits of Trotterization and the Taylor expansion leads to

$$\begin{aligned} \exp(-i\tilde{H}t + \tilde{L}t) = & \lim_{n \rightarrow \infty} \left( \left( \exp(-i\tilde{H}\frac{t}{n}) \right)^n \right) \\ & + \sum_j \gamma_j [\gamma_j \text{ terms}] \\ & + \sum_j \sum_k \gamma_j \gamma_k [\gamma_j \gamma_k \text{ terms}] + \dots, \end{aligned} \quad (9)$$

where we have used  $[\gamma_j \text{ terms}]$  to represent the (infinite) collection of terms all with  $\gamma_j$  as a prefactor. This represents the general (exact) evolution operator for our system. Our density matrix at time  $t$  can now be written

$$\begin{aligned} \tilde{\rho}(t) = & \lim_{n \rightarrow \infty} \left( \left( \exp(-i\tilde{H}\frac{t}{n}) \right)^n \right) \tilde{\rho}_0 \\ & + \sum_j \gamma_j [\gamma_j \text{ terms}] \tilde{\rho}_0 \\ & + \sum_j \sum_k \gamma_j \gamma_k [\gamma_j \gamma_k \text{ terms}] \tilde{\rho}_0 + \dots \end{aligned} \quad (10)$$

The first term of this expansion represents the noise-free result. Other terms represent the effects of noise on the evolution. Since this method directly corrects the density matrix,  $\rho$ , it follows that it also corrects an arbitrary observable,

$$\langle A \rangle = A_0 + \sum_j \gamma_j A_j + \sum_j \sum_k \gamma_j \gamma_k A_{jk} + \dots, \quad (11)$$

where  $A_0$  is the noise-free observable value and  $A_j$  is the effect of noise rate  $j$  on the observable. We define the ‘order’ of the combined Trotterization and Taylor expansion by the number of  $\gamma_j$  terms included. The first order terms, for example, are those with a single  $\gamma_j$  prefactor,

and include all possible ways that one (infinitesimal) error evolution can be included. The second order terms include all possible ways that two (infinitesimal) error evolutions can be included, and so on. We do not *a priori* know what the values of the effects of noise on the observable (such as  $A_j$ ) for any order are; however, we can characterize  $\gamma_j$  for a given experiment. By taking a sequence of experiments, varying  $\gamma_j$ , we can reconstruct the unknown evolution terms by fitting a hypersurface to the points. The coefficients of the hypersurface represent the effects (or, for the zeroth order term, the lack of effects) of noise to a given order on the density matrix (or an arbitrary observable). Equation (11) generally has effects up the infinite order; to make it tractable, we truncate at some given order. As more orders are included, the fit becomes more accurate, and, therefore, a better approximation of the noise-free result is obtained.

### Number of Terms in Expansion

Naively, the number of terms in a given order  $l$  would be  $m^l$ , where  $m$  is the number of noise terms (which could be the number of qubits or a small factor times the number of qubits). Since  $\gamma_j$  is a scalar, all  $\gamma_j$  will commute, allowing us to fuse terms with the same set of  $\gamma$ . For instance, given a second order expansion with two noise terms, we would general have terms with prefactors  $\gamma_1\gamma_1, \gamma_1\gamma_2, \gamma_2\gamma_1$ , and  $\gamma_2\gamma_2$ , but since  $\gamma_1\gamma_2 = \gamma_2\gamma_1$ , we can reduce the number of fitted parameters by combining the  $\tilde{L}_1\tilde{L}_2$  and  $\tilde{L}_2\tilde{L}_1$  terms. For a given order  $l$  and number of noise terms  $m$ , the number of parameters  $n$  for that order is the number of multinomial coefficients, which is given by the formula

$$n = \binom{l+m-1}{m-1}. \quad (12)$$

For an expansion truncated at order  $l$ , the total number of parameters, for all orders, is the sum of equation (12) for each order up to, and including,  $l$ .

- 
- [1] P. W. Shor, SIAM review **41**, 303 (1999).
  - [2] B. P. Lanyon, J. D. Whitfield, G. G. Gillett, M. E. Goggin, M. P. Almeida, I. Kassal, J. D. Biamonte, M. Mohseni, B. J. Powell, M. Barbieri, *et al.*, Nature chemistry **2**, 106 (2010).
  - [3] C. L. Degen, F. Reinhard, and P. Cappellaro, Reviews of modern physics **89**, 035002 (2017).
  - [4] M. A. Nielsen and I. L. Chuang, *Quantum computation and quantum information* (Cambridge university press, 2010).
  - [5] K. Temme, S. Bravyi, and J. M. Gambetta, Physical review letters **119**, 180509 (2017).



- [6] A. Kandala, K. Temme, A. D. Corcoles, A. Mezzacapo, J. M. Chow, and J. M. Gambetta, arXiv preprint arXiv:1805.04492 (2018).
- [7] M. Otten and S. K. Gray, arXiv preprint arXiv:1804.06969 (2018).
- [8] M. Otten, R. A. Shah, N. F. Scherer, M. Min, M. Pelton, and S. K. Gray, Physical Review B **92**, 125432 (2015).
- [9] M. Otten, J. Larson, M. Min, S. M. Wild, M. Pelton, and S. K. Gray, Physical Review A **94**, 022312 (2016).
- [10] M. Otten, “QuaC: Open quantum systems in C, a time-dependent open quantum systems solver,” <https://github.com/Ott3r/QuaC> (2017).
- [11] M. Reagor, C. B. Osborn, N. Tezak, A. Staley, G. Prawiroatmodjo, M. Scheer, N. Alidoust, E. A. Sete, N. Didier, M. P. da Silva, *et al.*, Science advances **4**, 3603 (2018).
- [12] R. S. Smith, M. J. Curtis, and W. J. Zeng, arXiv preprint arXiv:1608.03355 (2016).
- [13] C. Müller, J. Lisenfeld, A. Shnirman, and S. Poletto, Physical Review B **92**, 035442 (2015).
- [14] H. Paik, D. Schuster, L. S. Bishop, G. Kirchmair, G. Catelani, A. Sears, B. Johnson, M. Reagor, L. Frunzio, L. Glazman, *et al.*, Physical Review Letters **107**, 240501 (2011).
- [15] S. F. Huelga, C. Macchiavello, T. Pellizzari, A. K. Ekert, M. B. Plenio, and J. I. Cirac, Physical Review Letters **79**, 3865 (1997).
- [16] F. Jelezko, T. Gaebel, I. Popa, M. Domhan, A. Gruber, and J. Wrachtrup, Physical Review Letters **93**, 130501 (2004).
- [17] R. Uzdin, A. Levy, and R. Kosloff, Physical Review X **5**, 031044 (2015).
- [18] H. F. Trotter, Proceedings of the American Mathematical Society **10**, 545 (1959).